Effect of mould inoculation on formation of chunky graphite in heavy section spheroidal graphite cast iron parts

I. Asenjo[1], P. Larrañaga[1], J. Sertucha[1], R. Suárez[1], J.-M. Gómez[2], I. Ferrer[2] and J. Lacaze*[3]

The manufacturing process of heavy section ductile iron castings is strongly influenced by the risk of graphite degeneration under slow cooling rates. Appearance of this kind of defect is commonly linked to significant reductions in the mechanical properties of large castings. Studies on the effect of inoculation on chunky graphite formation in heavy sections have led to contradictory results in the literature and this triggered the present work. New experimental data are presented on the effect of mould inoculation on chunky graphite appearance during solidification of nodular irons which clearly demonstrate that mould inoculation increases the risk of chunky graphite formation in heavy sections. This is in agreement with some previous works which are reviewed, and it is suggested that the contradiction with other results could relate to the fact that these latter works dealt with chill casting.

Keywords: Spheroidal graphite cast iron, Heavy section casting, Mould inoculation, Graphite degeneracy, Chunky graphite

Introduction

Chunky graphite, denoted CHG in the following, has been recognised for a long time as one of the major problems when casting large parts in nodular cast irons[1] and has been the subject of several reviews.[2–5] It may be mentioned here that CHG was often called vermicular graphite until late 1970s. Javaid and Loper[4] made a complete review of the factors affecting graphite formation in production of heavy section ductile cast iron, putting emphasis on melt chemistry. They differentiated alloying elements, additions and impurities and detailed their effect or counter effect on graphite degeneracy. The review by Källbom *et al.*[5] is somehow less extensive but covers more recent work and presents some attempts to rationalise the experimental knowledge on CHG formation. As a matter of fact, both reviews showed that many results reported about this phenomenon seem contradictory, to mention a few:

(i) importance of purity of the initial charge
(ii) effect of pouring temperature
(iii) timing of the formation of CHG during the solidification sequence
(iv) effect of inoculation.

As the present work was aimed at studying the effect of mould inoculation on CHG formation, a more detailed review of the results available so far on that peculiar aspect was carried out. It is of some interest to mention the only three sentences on 'chunk' graphite found in the ASM specialty handbook:[6] 'large interconnected graphite cells, possibly with nodules at intercellular boundaries (similar to ASTM type V graphite). Most commonly associated with heavy sections and slow solidification rate. Low nodule counts and increasing magnesium levels minimise the formation of chunk graphite'. The importance of proper handling of magnesium level and nodule counts was also stressed in the review by Javaid and Loper[4] who discussed fading of spheroidising and inoculation treatments, emphasising however that they occur independently. Similar to the ASM handbook, Javaid and Loper noted that fading of Mg should lead to vermicular (though not mentioning CHG) and eventually flake graphite and proposed to decrease as much as possible the time for melt handling. On the contrary, their conclusions on inoculation and nodule count are opposite to those of the ASM handbook and they suggested using late inoculation to ensure a minimum nodule count of 60–70 mm^{-2} to avoid CHG formation.

This conclusion on the beneficial effect of the nodule count was based on earlier studies[7–10] on the use of chills and directional solidification. Contrary to Kust and Loper[7] and Basutkar *et al.*[8,9] who concluded that the CHG risk decreased with an increase in nodule count, Buhr[10] did not find any beneficial effect in elimination of CHG graphite (though called vermicular graphite in this work) by increasing the amount of inoculant in chill

[1]Engineering and Foundry Department, Azterlan, Aliendalde auzunea 6, E 48200 Durango (Bizkaia), Spain
[2]TS Fundiciones, SA Pol. Sansinenea Erreka, E 20749 Arroa-Zestoa (Gipuzkoa), Spain
[3]CIRIMAT, UMR 5085 CNRS/UPS/INPT, ENSIACET, 31077 Toulouse cedex 4, France

*Corresponding author, email jacques.lacaze@ensiacet.fr

Received 29 October 2007; accepted 11 March 2008
DOI 10.1179/136404608X286138

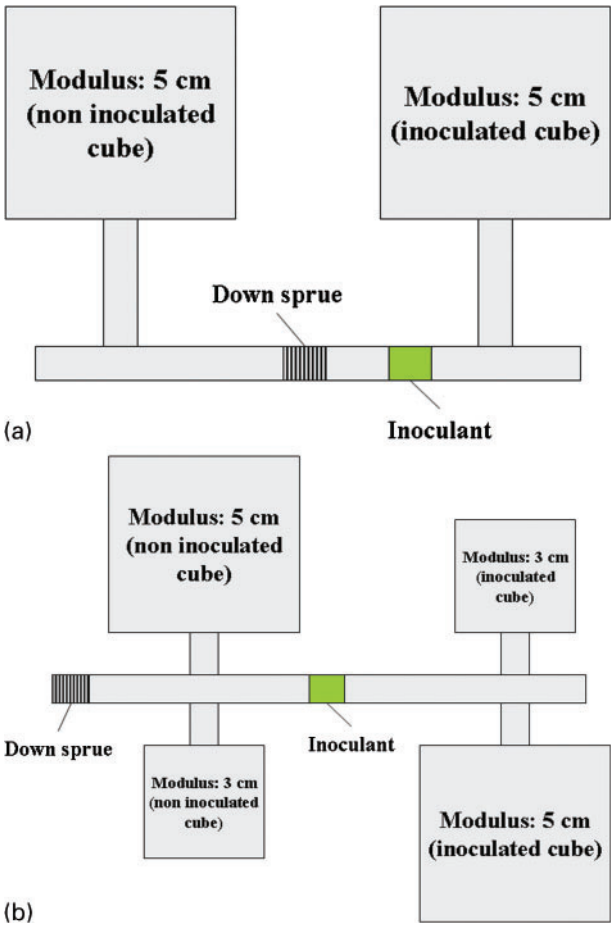

1 Patterns used in experiments, with either *a* two or *b* four blocks

casting. Concerning sand casting without chills, two detailed reports on the effect of nodule count on CHG formation are available[11,12] that both show an increase of graphite degeneracy with an increase in nodule count. As part of a study devoted to controlling the melt quality of heavy section castings, it appeared of significant interest to investigate again the effect of inoculation and nodule count. A series of large block castings that were either or not mould inoculated was selected for that purpose, with the hope of shedding some light on the above contradiction on the relation between nodule count and CHG appearance.

Experimental

The test castings used in this study were cubic blocks, 180 and 300 mm in size, that have thermal moduli (ratio of the volume of the casting to its outer surface available for heat transfer) of 3 and 5 cm respectively. The moulds were produced from furan sand and positioned inside metal boxes about $1000 \times 1000 \times 350$ mm for the bottom part and $1000 \times 1000 \times 400$ mm for the top part. Two different patterns were used depending on the number of blocks, either two or four as illustrated in Fig. 1. In order to investigate the influence of inoculation, pairs of blocks with and without inoculation were always cast at the same time. Inoculation was performed by adding $\sim$0·20% of the weight of the metal of a commercial inoculant in the form of ingots fixed with a foundry adhesive in the gating system as indicated in the schematics of Fig. 1. The inoculant composition was 70–78Si, 3·2–4·5Al, 0·3–1·5Ca and $\sim$0·5RE (wt-%).

In order to differentiate the various cubes that were cast, they will be denoted MX-Y-I or MX-Y-N where:

(i) MX defines the thermal modulus of the cube (M3 or M5)
(ii) Y is the experiment number (1, 2, 3 ...)
(iii) I and N indicate either inoculated (I) or non-inoculated (N) block.

Melts were prepared in medium frequency induction furnaces of 10 and 15 t capacity from pig iron and automotive steel scrap as listed in Table 1. For limiting the number of parameters, effort was made to use melts with very similar compositions and processing conditions. Once melting was finished, the chemical composition of the metal was adjusted according to carbon evaluation given by thermal analysis using the Thermolan system[13,14] and to spectrometry analysis on a coin sample for the other elements. If it was necessary, the carbon content was increased by adding electrode graphite while FeSi 75% was used for silicon. The amount of the other elements was expected to be so low that no adjustment was needed. Besides, two different conditioners (or pre-inoculants) have been used in order to increase the nucleation ability of the melt, SiC and a commercial alloy based on $FeSi_2$ (Fe–63·0Si–8·3Ba–1·4Al–0·13Ca, wt-%). The SiC is normally added into the furnace with the metallic charge whereas the $FeSi_2$ alloy is added at the end of the melting procedure.

In all experiments, the spheroidising treatment was carried out at $\sim$1430°C by adding FeSiMg alloy (45·0Si–9·1Mg–2·8Ca–1·1RE– 0·9Al, wt-%) using the sandwich method. The FeSiMg alloy was positioned at the bottom of the casting ladle and then covered by steel scrap before pouring the iron from the furnace. Table 2 lists all the additions made for spheroidisation. After the treatment, slag was removed from the melt surface and the iron was poured directly into the mould at a temperature of about 1380–1400°C.

Just before pouring the iron in the mould, a metal sample was taken that was analysed by combustion techniques using a Leco CS 244 equipment for determining C and S contents, inductively coupled

Table 1 Metallic charges used in melting area

	Materials, kg					
Trial	Pig iron	Steel scrap	Electrode graphite	FeSi 75%	SiC	$FeSi_2$
1	5600	1900	43	83	45	30
2	10 500	3600	80	213	91	56
3	2585	2215	62	52	21	24
4	2640	2160	60	56	22	24
5	7450	4100	100	248	107	58
6	9900	3600	77	208	86	47

Table 2 Materials used in spheroidisation treatments, kg

Trial	Treated iron	FeSiMg	Steel cover
1	7700	58	77
2	4200	27	42
3	4960	39	50
4	4900	41	49
5	4300	27	43
6	4500	30	45

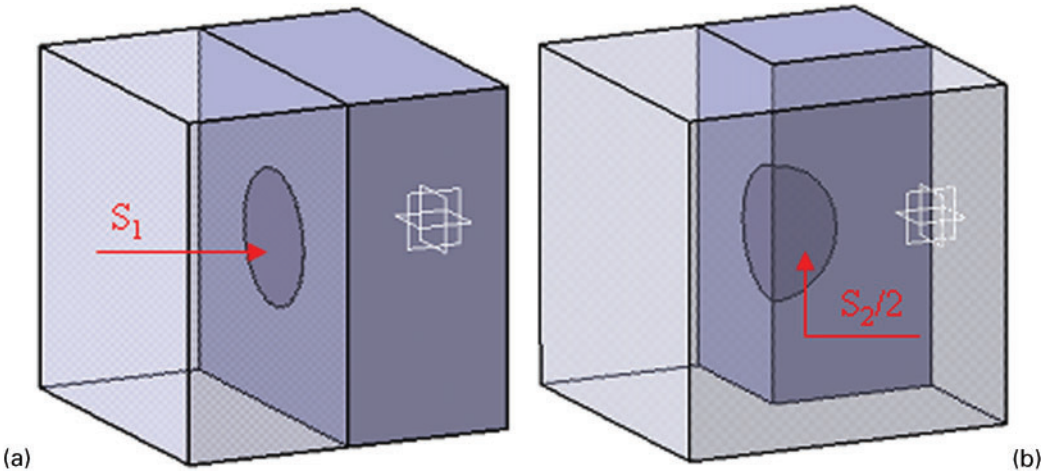

2 Schematics showing cuts made through blocks with definition of areas *a* S_1 and *b* $S_2/2$ used to evaluate zones affected by CHG

plasma and mass spectrometry (ICP-MS Agilent 7500ce) for Sb, Pb and Ce, and optical emission spectrometry (OBLF QS750) for Si, P, Cu, Cr, Ni, Mn and Mg. The results of the chemical analysis are listed in Table 3, with an indication of the accuracy for each element. Note that the slight increase in silicon related to post-inoculation is not accounted for in the values listed.

At the time of pouring, two standard cups for thermal analysis were also filled and their cooling curves recorded using Thermolan system. One of the cups contained ~0·20% of the standard sample mass of the same inoculant as used for the blocks. The inoculant added to the cups was obtained by grinding an ingot of inoculant and sifting the resulting powder to select particles from 0·2 to 0·7 mm. The cooling curves were then analysed following the procedure described elsewhere[13,14] so as to determine the eutectic temperatures and to obtain estimated nodule counts that will be denoted N_{therm} in the following.

Each block was afterwards sectioned (Fig. 2*a*) parallel to one of its vertical symmetry plans, and one of the halves was cut again to give a section along the second vertical symmetry plan (Fig. 2*b*). As illustrated by the macrograph in Fig. 3, the area affected by CHG was generally easily located as the darker zone in the centre of the sections. A macrograph of the sections was then taken and the areas affected by chunky graphite were estimated by means of the commercial image analysis software Image J. Denoting S_1 the area affected by CHG in the first section, and $S_2/2$ the one in the half second section (*see* Fig. 2), an evaluation of the volume V of the CHG zone was made by means of the expression $V = \frac{2}{3\pi^{1/2}}\left(S_1 S_2^{1/2} + S_2 S_1^{1/2}\right)$ which assumes an ellipsoid shape. This value was then normalised with the volume of the related block to give the fraction of the volume V_V affected by CHG.

Also, samples obtained from the geometrical centre of the blocks were prepared for metallographic analysis by means of optical microscopy. Figure 4 presents examples of the micrographs obtained with different levels of CHG. The specific surface A_A of areas affected by CHG was evaluated using Image J software and the average of measurements performed on five different fields was used to characterise each block. On the same sample, the nodule count N_{block} was evaluated using Leica image analysis software by measuring it on different micrographs obtained at an enlargement of $\times 100$ in areas where the graphite was correctly formed. Only particles with area larger than 20 μm^2 (~ 5 μm in diameter) were considered as graphite nodules. Again, the value N_{block} for each block was obtained as the average of the measurements performed in those five fields.

Results

Table 4 lists the results of the fractions V_V and A_A affected by CHG, as well as the experimental N_{block} and evaluated N_{therm} nodule counts.

The detection of the zone affected by CHG on the sections of the blocks was usually easy because of the marked change of contrast. In a few cases, the limits of this zone were made more precise by optical microscopy. Chunky graphite appeared in all the inoculated M3 blocks but not in the non-inoculated M3 ones. In the case of M5 castings, CHG appeared in both inoculated and non-inoculated blocks, but with higher V_V values in the inoculated ones as evidenced by the data in Table 4. It was also noted that the larger the cast part, the bigger the volume fraction affected by CHG. Microscopic

Table 3 Chemical composition of melts, wt-%: numbers between brackets in first row give accuracy for each element

Trial	$C_{(0·06)}$	$Si_{(0·02)}$	$P_{(0·004)}$	$S_{(0·001)}$	$Cu_{(0·005)}$	$Cr_{(0·002)}$	$Ni_{(0·007)}$	$Mn_{(0·01)}$	$Mg_{(0·004)}$	$Sb_{(0·0002)}$	$Pb_{(0·0002)}$	$Ce_{(0·0002)}$
1	3·64	2·40	0·038	0·011	0·01	0·02	0·01	0·10	0·045	<0·0002	<0·0002	0·0024
2	3·72	2·35	0·034	0·007	0·01	0·02	0·01	0·10	0·036	<0·0002	<0·0002	0·0023
3	3·61	2·28	0·036	0·009	0·01	0·02	0·01	0·20	0·043	<0·0002	<0·0002	0·0027
4	3·65	2·23	0·039	0·013	0·01	0·02	0·01	0·21	0·052	<0·0002	<0·0002	0·0025
5	3·64	2·19	0·036	0·012	0·02	0·02	0·01	0·17	0·041	<0·0002	<0·0002	0·0023
6	3·72	2·20	0·039	0·011	0·02	0·02	0·01	0·10	0·040	<0·0002	<0·0002	0·0028

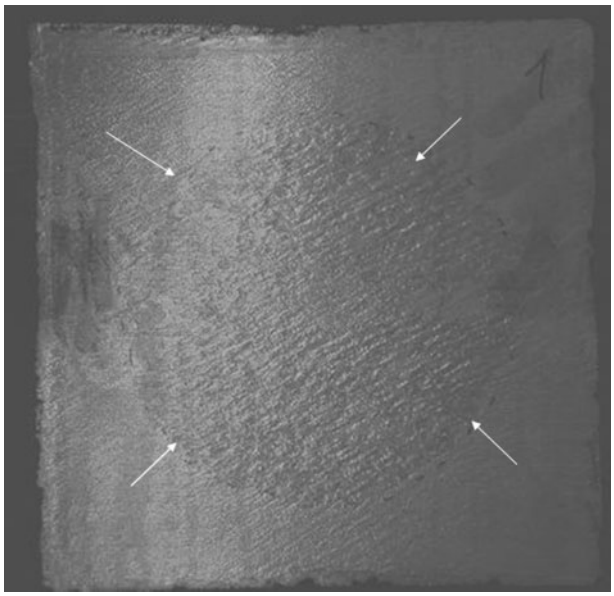

3 Central section of cast block with zone affected by CHG appearing with darker contrast

observations showed that CHG grows as eutectic cells (Fig. 4) with apparent diameter in the range 0·5 to 1 mm in M3 blocks and 0·5 to 2·5 mm in M5 blocks. Figure 5 shows V_V versus A_A experimental values. In the case of the M5 blocks, it is noteworthy that low values of A_A may be associated with high values of V_V and vice versa. Such an observation could mean that when the volume affected by CHG is small, graphite degeneracy is concentrated at the very centre of the block with higher relative A_A values. On the contrary, when V_V is high, it has been observed that the centre of the block is sometimes free from CHG. Such a distribution of CHG areas in the blocks would lead to the tendency that V_V decreases when A_A increases, but such a relationship could hardly be inferred from Fig. 5 because of the scatter of the data. Also, this conclusion does not seem

Table 4 Experimental nodule counts N_{block}, estimated nodule counts N_{therm}, volume fractions V_V and area fractions A_A at centre of blocks affected by CHG

Trial	Code	N_{block}, mm^{-2}	N_{therm}, mm^{-2}	V_V, %	A_A, %
1	M5-1-I	70	328	29	1
	M5-1-N	25	180	5	22
2	M5-4-I	70	240	9	7
	M5-4-N	40	212	8	1
	M3-4-I	130	240	1	12
	M3-4-N	60	212	0	1
3	M5-5-I	70	270	16	13
	M5-5-N	25	115	1	37
	M3-5-I	135	270	3	14
	M3-5-N	30	115	0	0
4	M5-6-I	65	333	24	20
	M5-6-N	25	141	2	42
	M3-6-I	175	333	3	11
	M3-6-N	35	141	0	0
5	M5-10-I	85	262	16	27
	M5-10-N	40	213	11	7
6	M5-11-I	80	261	14	24
	M5-11-N	35	106	7	11

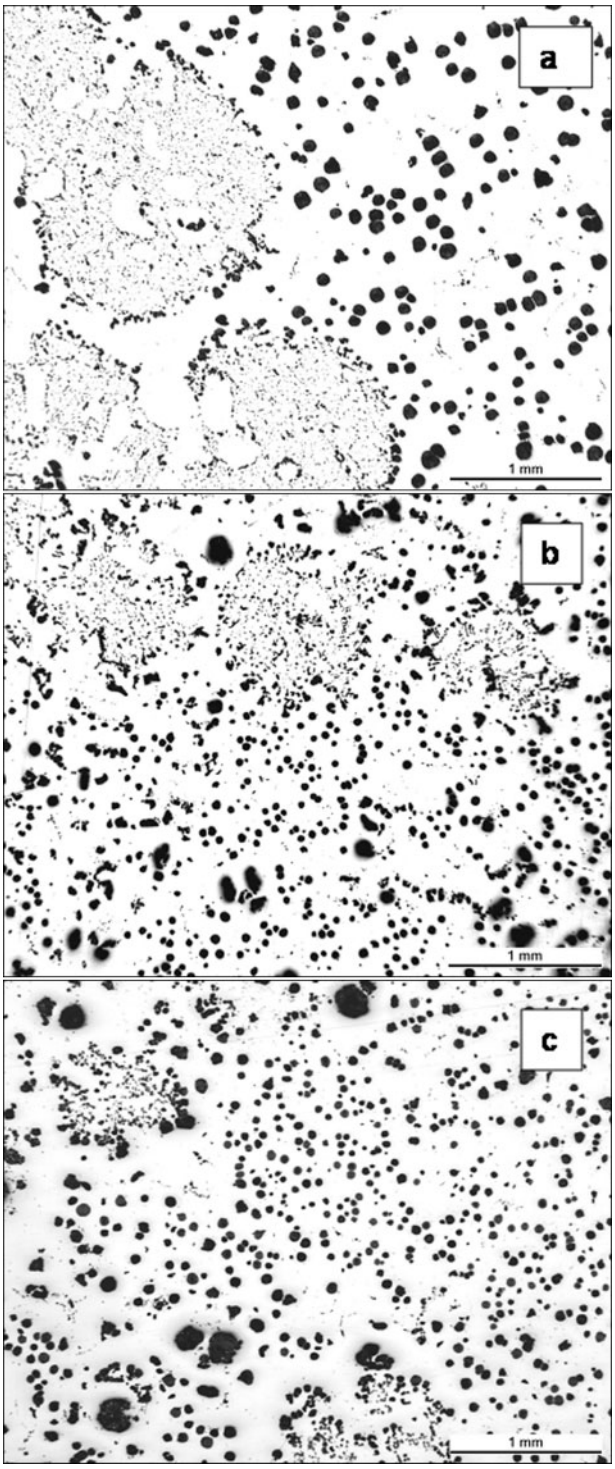

a block M5-6-N, A_A=42% and V_V=2%; *b* block M5-5-I, A_A=13% and V_V=16%; *c* block M5-4-I, A_A=7% and V_V=9%

4 Optical micrographs obtained from central zone of different blocks showing various amounts of CHG

to apply to M3 blocks on the basis of the very few data available. Considering that the area fraction of CHG is generally not uniform within the affected zone, it seemed more relevant to use V_V as the best quantity to characterise graphite degeneracy in practice, in agreement with most previous works.

As expected, the nodule counts reported in Table 4 show higher numbers of spheroids with post-inoculation of either M3 or M5 blocks, as well as for the smaller M3

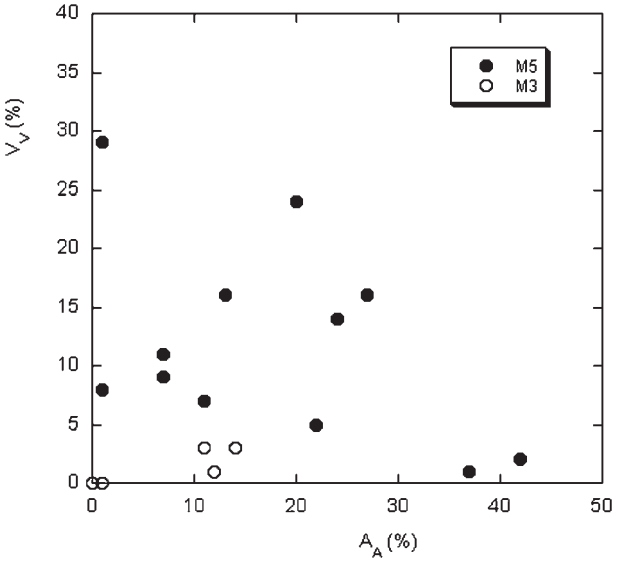

5 Relation between V_V and A_A values

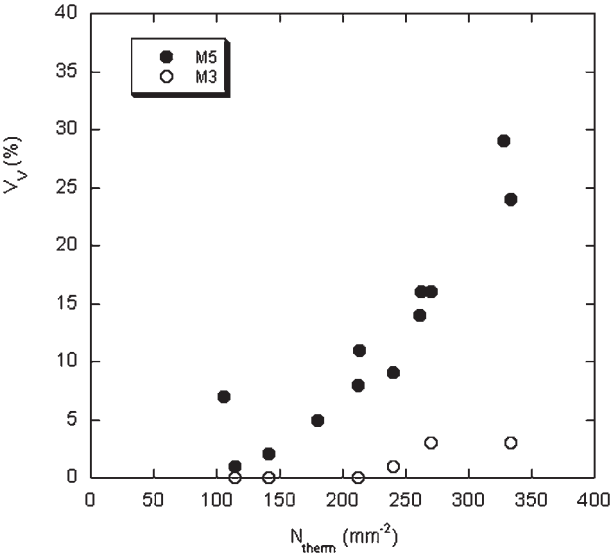

7 Relation between V_V and N_{therm}

blocks when compared to the M5 ones. Figure 6 shows a strong relationship between the nodule counts measured on the blocks, N_{block}, and those estimated from the thermal analysis cups, N_{therm} (note in Table 4 that the same N_{therm} values have been used for M3 and M5 in the case of four block castings). As expected, M3 blocks give rise to higher nodule counts than M5 ones because of their smaller modulus, but it is seen in Fig. 6 the difference becomes evident at high nodule counts only. Rather than using the nodule counts measured in the area affected by CHG, Karsay and Campomanes[11] used a reference nodule count measured in the bottom corner of the blocks, i.e. outside the affected zone. They suggested that any kind of casting with reproducible cooling rates could be used as reference. Accordingly, the nodule count estimated from thermal analysis records may be used as reference as conducted in the following.

Finally, the V_V values are plotted against the corresponding values of the reference nodule count N_{therm} in Fig. 7. For both M3 and M5 castings, it can be observed that the volume affected by CHG increases with the number of nodules.

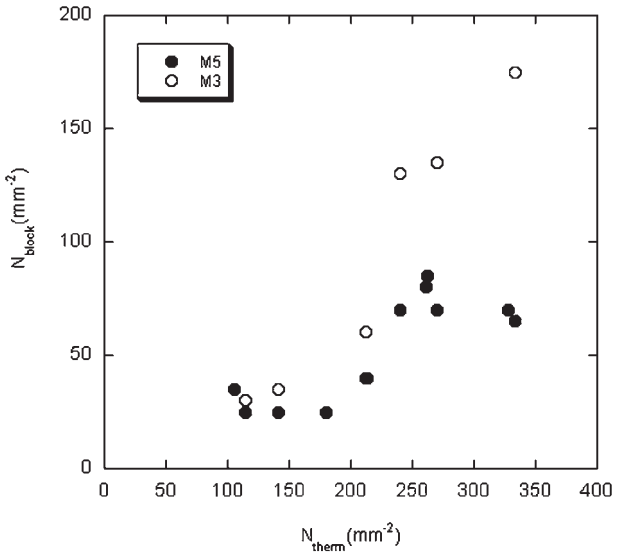

6 Relation between N_{block} and N_{therm}

Discussion

It is thus clearly established that an increase in the nodule count is associated with an increase in the volume affected by CHG in castings of a melt prone to graphite degeneracy. This applies to sand castings with large modulus in industrial conditions and agrees with the conclusion of previous detailed studies mentioned in the introduction.[11,12] This is also in line with more limited observations as those reported by Gagné and Argo[15] who found that doubling the amount of post-inoculation failed to suppress CHG formation in 20 cm diameter cylinders while very strong post-inoculation of 3·2 cm diameter cylinders made some CHG appear. In Fig. 8 the V_V values measured during this study are plotted against the N_{block} values, together with the data from Karsay and Campomanes for their MgFeSi treated

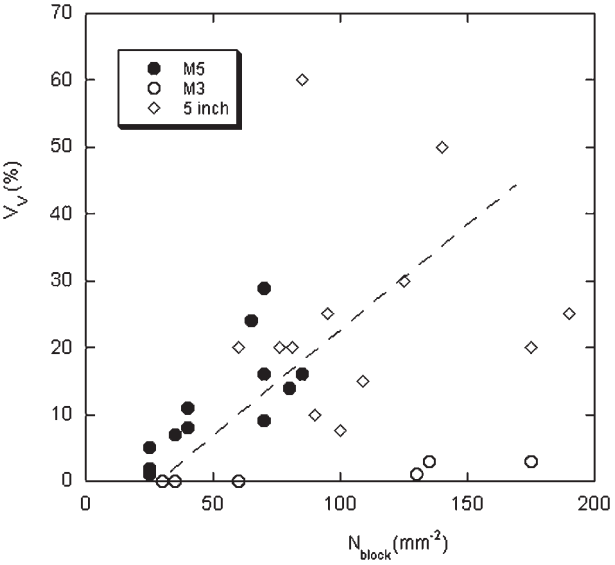

8 Experimental relation between V_V and N_{block} from this study (M3 and M5) and from Karsay and Campomanes[11] for their cubic casting 127 mm in size (label 5 inch in figure): line is from this latter work

melts,[11] considering only castings without Sb treatment (commonly used as inhibitor to CHG formation). Though the scatter of these latter results is high, the authors could draw the line reproduced in Fig. 8 to stress the tendency they observed. It seems noteworthy to mention that the values from the present study are in an overall very good agreement with those from Karsay and Campomanes.

Cooling curves recorded at the centre of the blocks, to be described elsewhere, showed features like those previously reported in similar studies, e.g. by Buhr,[10] with a very long eutectic plateau with limited recalescence. In contrast, directional solidification as obtained by casting on chills is characterised by cooling curves with a continuous decrease of the metal temperature at locations close enough to the chill.[9,10] In those locations, the eutectic reaction proceeds at continuously increasing undercooling, a situation which is known to favour spheroidal growth against degenerate forms.[1,16] As the distance to the chill increases further, a eutectic plateau appears which becomes more and more pronounced and lengthy. One may suggest that it is in those locations that Kust and Loper[7] and Basutkar *et al.*[8] observed CHG, and this relates to a dramatic decrease of the temperature gradient reported by Pan *et al.*[17] who unfortunately did not give details of the method for estimating it. This seems to be confirmed in the work by Basutkar *et al.*[9] who reported CHG to form only in non-Ce treated melts at distances higher than 150 mm (6 inch in the original publication) from the chill, i.e. in all cases close to the thermal centre of their castings. The formation of CHG would thus not be due to the decrease of the nodule count, this latter being an effect of the decrease in the cooling rate,[10] but to the fact that the eutectic reaction proceeds at nearly constant temperature in much the same conditions than during sand casting. It would thus be of great interest to get more precise data on the formation of CHG in chill casting, namely to have the volume of CHG and the nodule count versus the distance to the chill as well as precise information about the cooling curves. If the present analysis is correct, i.e. that the conditions of CHG formation far from the chill surface are similar to those encountered in sand casting, the controversy on the effect of nodule count on CHG formation recalled in the introduction would thus be simply an artefact of presentation.

Conclusions

This study has demonstrated the usefulness of casting blocks with moduli of 3 and 5 cm for investigating graphite degeneracy in heavy section castings. As a matter of fact, it was observed that castings with 5 cm modulus contain much larger amounts of chunky graphite than those with a thermal modulus of 3 cm. This size effect demonstrates the influence of the cooling conditions on formation of chunky graphite. In all cases, chunky graphite appeared in the central part of the castings, concentrated in the very centre of the casting when the amount of CHG was low, quite dispersed over large affected areas in the opposite case.

The most important result of this study is that mould inoculation increased the amount of chunky graphite in blocks with modulus equal either to 5 or to 3 cm. Mould inoculation leads to higher nodule counts and it was found appropriate to use the nodule count estimated on thermal cups as reference value, in much the same way than previously suggested. This detrimental effect of increased nodule count agrees with other previous works carried out on sand castings, but is at change with some other reports that all dealt with chill castings. It is proposed that this discrepancy relates to the difference in the cooling conditions, chill casting leading to a continuous cooling of the metal whilst sand casting of large sections is characterised by lengthy eutectic plateaus at nearly constant temperature.

Acknowledgement

This paper is based on work supported by the Industry Department of the Spanish Government (grant nos. PROFIT FIT-030000-2007-94 and CDTI IDI-20060574).

References

1. R. Elliott: in 'Cast iron technology', 99; 1988, London, Butterworths.
2. E. Campomanes: *Giesserei*, 1978, **65**, 535.
3. H. W. Hoover: *AFS Trans.*, 1986, **94**, 601.
4. A. Javaid and C. R. Loper, Jr: *AFS Trans.*, 1995, **103**, 135.
5. R. Källbom, K. Hamberg and L.-E. Björkegren: Proc. Gjutdesign 2005 Final Semin., Espoo, Finland, June 2005, VTT Technical Resarch Centre of Finland.
6. in 'ASM specialty handbook', (ed. J. R. Davis), 297, 'Cast irons'; 1996, Materials Park, OH, ASM International.
7. R. R. Kust and C. R. Loper, Jr: *AFS Trans.*, 1968, **76**, 540.
8. P. K. Basutkar, C. R. Loper and C. L. Babu: *AFS Trans*., 1970, **78**, 429.
9. P. K. Basutkar, C. R. Loper, Jr: *AFS Trans*., 1971, **79**, 176.
10. R. K. Buhr: *AFS Trans*., 1968, **76**, 497.
11. S. I. Karsay and E. Campomanes: *AFS Trans*., 1970, **58**, 85.
12. Z. Ignaszak: *Int. J. Cast Met. Res*., 2003, **16**, 93.
13. R. Suárez: Proc. 1st Symp., 'Azterlan and the foundry sector', Bilbao, Spain, July 2002, 1–7.
14. P. Larrañaga, J. M. Gutiérrez, A. Loizaga, J. Sertucha and R. Suárez: *AFS Trans*., to be published.
15. M. Gagné and D. Argo: Proc. Int. Conf. on 'Advanced casting technology', (ed. J. Easwaren), 231; 1987, Materials Park, OH, ASM.
16. I. Minkoff: 'The physical metallurgy of cast iron'; 1983, New York, John Wiley and sons.
17. E. N. Pan, C. N. Lin and H. S. Chiou: *AFS Trans*., 1995, **103**, 265.